

Visual and Ratiometric Fluorescent Probe via An Intramolecular Charge Transfer for Detection of A Nerve Agent Simulant in Solutions and in Gas Phase

Anirban Karak^a, Shilpita Banerjee^a, Satyajit Halder^b, Mousmi Mandal^a, Dipanjan Banik^a, Anwesha Maiti^a, Kuladip Jana^b, Ajit Kumar Mahapatra^{a*}

^a *Molecular Sensor and Supramolecular Chemistry Laboratory, Department of Chemistry, Indian Institute of Engineering Science and Technology, Shibpur, Howrah 711 103, India*

^b *Division of Molecular Medicine, Bose Institute, P 1/12, CIT Scheme VIIM, Kolkata 700054, India.*

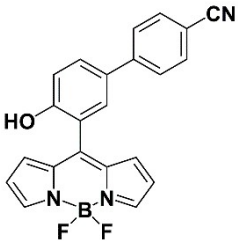
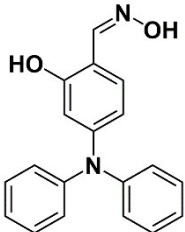
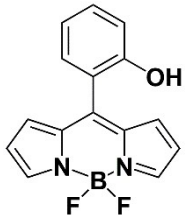
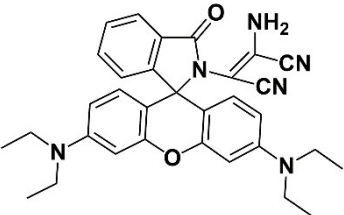
*Author to whom correspondence should be addressed; electronic mail:

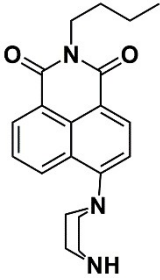
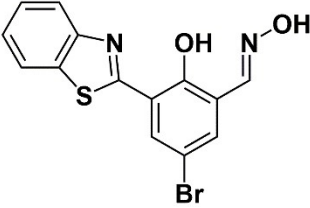
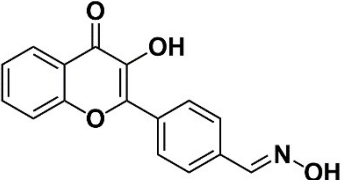
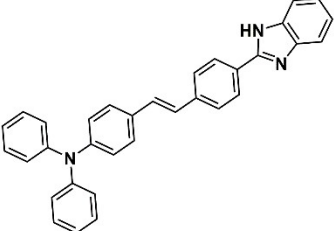
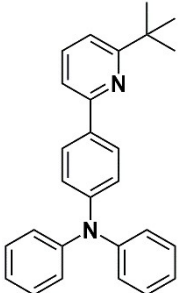
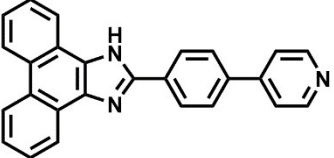
akmahapatra@chem.iiests.ac.in; Tel.: +91 – 9434508013

Table of Contents

1. Comparison table of previously reported DCP sensing probe with our present work
2. Quantum chemical DFT method
3. ESI-MS Spectra
4. NMR Spectra: ¹H NMR, ¹³C NMR
5. Calculation of detection limit
6. pH study
7. Response time
8. Spectral study of CC1
9. HRMS spectra of the adduct and controlled compound and ¹H NMR of controlled compound
10. Crystal Data and Structure Refinement Parameters
11. Cell line study
12. References

Table S1: Comparison table of previously reported DCP sensing probe with our present work

Structure of the probe	Solvent	Mode of sensing	Application	LOD	Response time	Ref
	DMF	PET	Paper strip detection	20.7 ppb		1
	CH ₃ CN–H ₂ O (4:6 v/v)	PET	Detection in vapor phase, soil sample, live cells	0.14 μM	30 s	2
	DMF	PET	Solid-State Detection	0.71 μg/L		3
	DCM (with 3% Et ₃ N)		Test strip detection	0.2 μM		4

	DMF	PET	Vapor phase detection	5.5 nM		5
	DMF	PET and ESIPT	Detection in vapor phase, soil sample, live cells	33.5 nM.	45 sec	6
	MeOH	Suppressing the intramolecular rotation	Test strip detection	7.8×10^{-7} mol L ⁻¹ .	90 sec	7
	THF/H ₂ O (4/1, v/v)	ICT	Vapor phase detection	8.45×10^{-8} M		8
	THF	ICT	Vapor phase detection	2.6 ppb	25 s	9
	DMSO-H ₂ O (2:3, v/v)	ICT	Vapor phase detection and detection in Live cells	1.4×10^{-9} M	18 s	Our probe

2. Theoretical calculations:

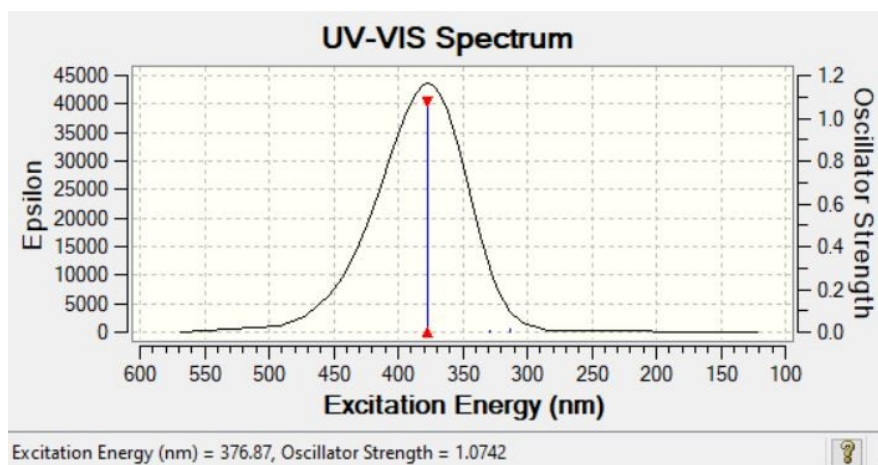


Figure S1. Absorption spectra of the Probe

Table S2: The vertical main orbital transition of the **Probe** calculated by TDDFT method

Energy (eV)	Wave length (nm)	Osc. strength (f)	Transition
3.2898	376.87	1.0742	HOMO→LUMO
3.7626	329.51	0.0060	HOMO→LUMO+1
3.9581	313.24	0.0178	HOMO-1→LUMO

Table S3: The vertical main orbital transition of the **Product** calculated by TDDFT method

Energy (eV)	Wave length (nm)	Osc. strength (f)	Transition
2.3093	536.89	0.9181	HOMO→LUMO
2.9128	425.65	0.0108	HOMO-1→LUMO
3.5451	349.73	0.2196	HOMO-2→LUMO

3. ESI-MS Spectra:

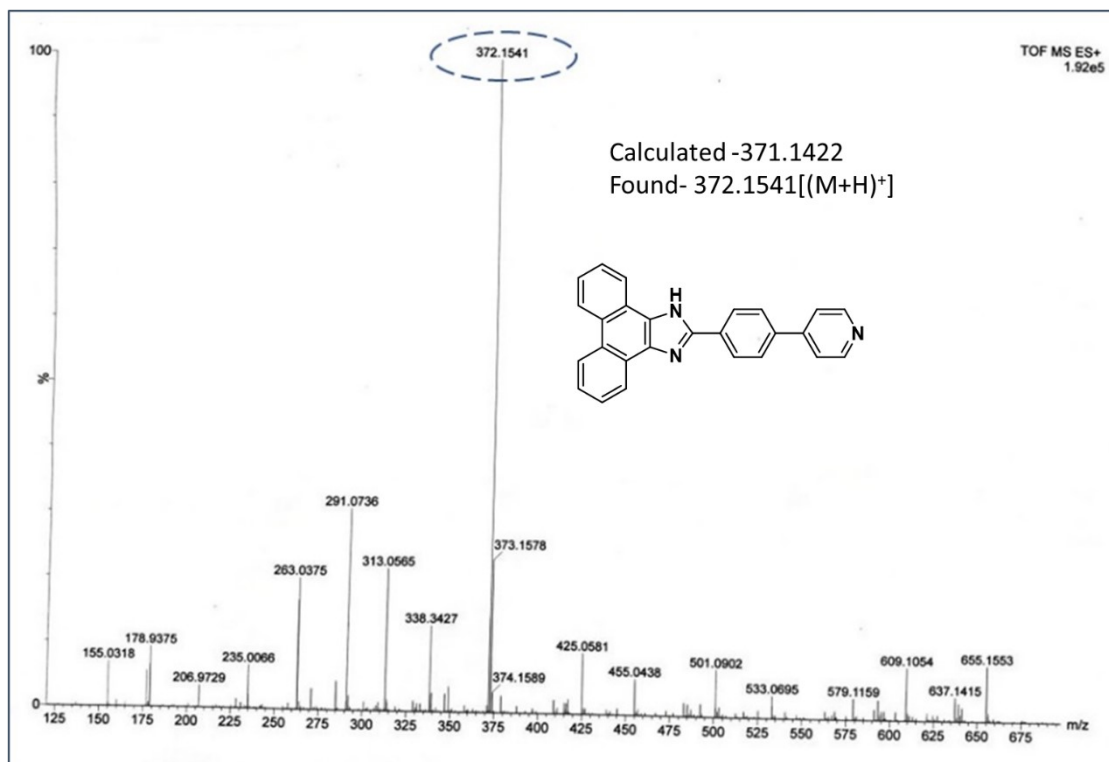


Figure S2: HRMS of the probe PPID

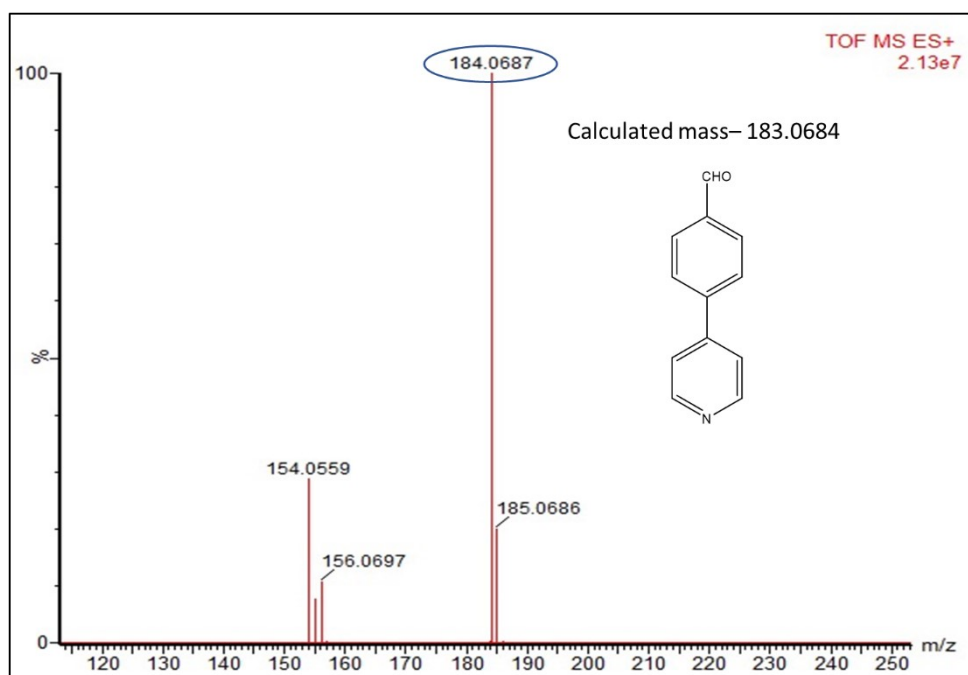


Figure S3: HRMS of the probe FPY

4. NMR Spectra: ¹H NMR, ¹³C NMR:

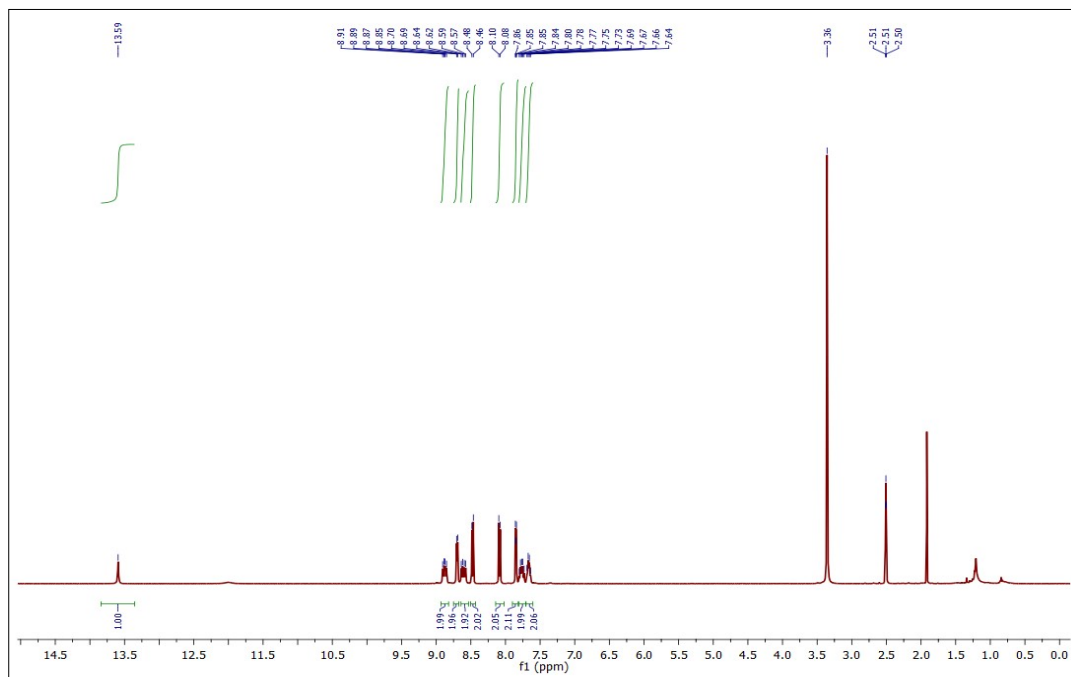


Figure S4: ¹H NMR of the probe PPID

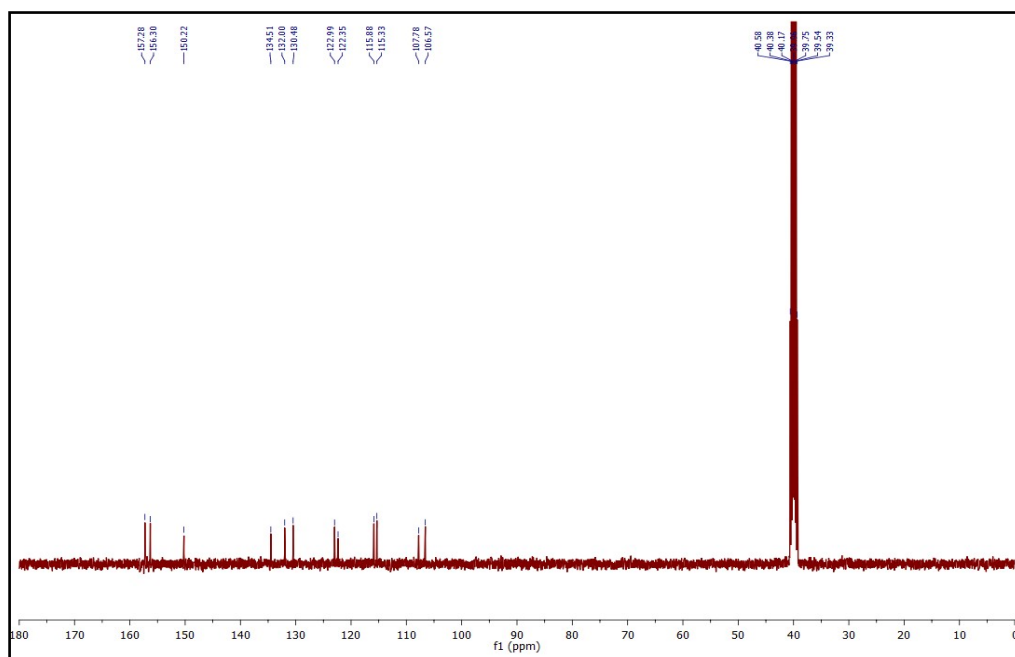


Figure S5: ¹³C NMR of the probe PPID

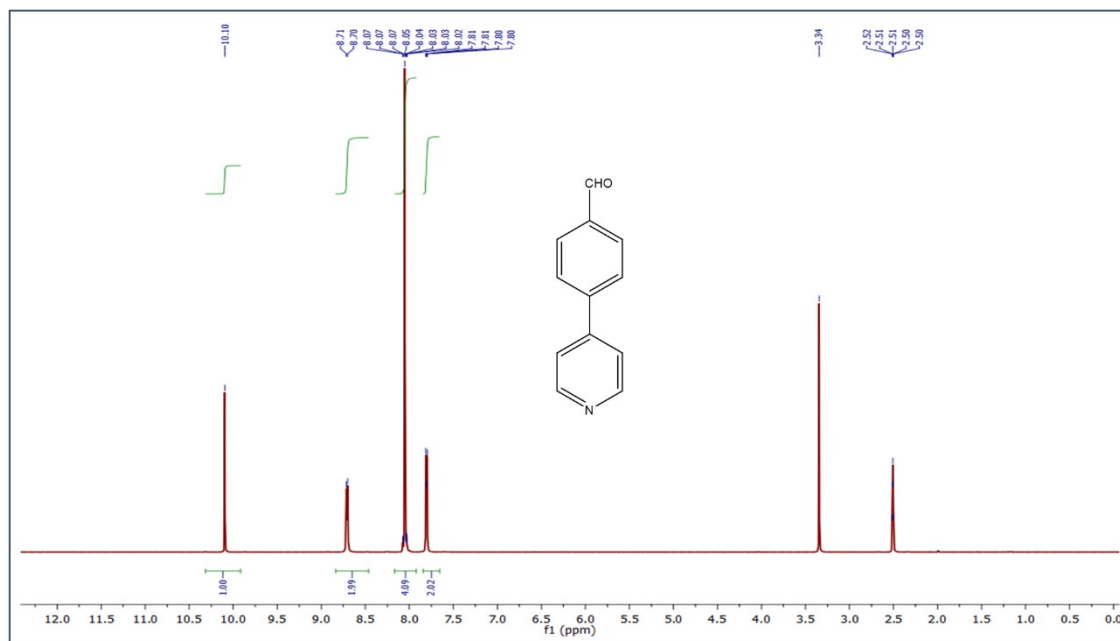


Figure S6: ^1H NMR of the aldehyde FPY

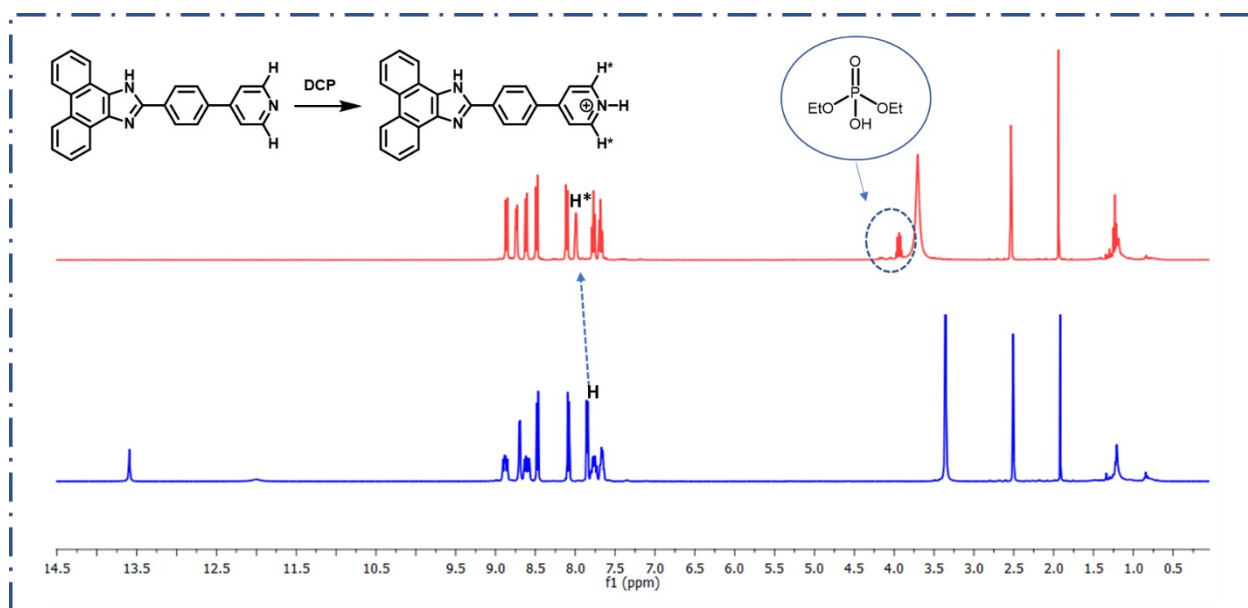


Figure S7: ^1H NMR titration of PPID with DCP

5. Calculation of detection Limit

The limit of detection (LOD) of PPID for DCP was calculated utilizing the general equation $DL = K \times Sb1/S$

Where $K = 2$ or 3 (we take 3 in this case) and $Sb1$, obtained as 3.25×10^{-4} is the standard deviation of the blank solution and S is the slope of the calibration curve.

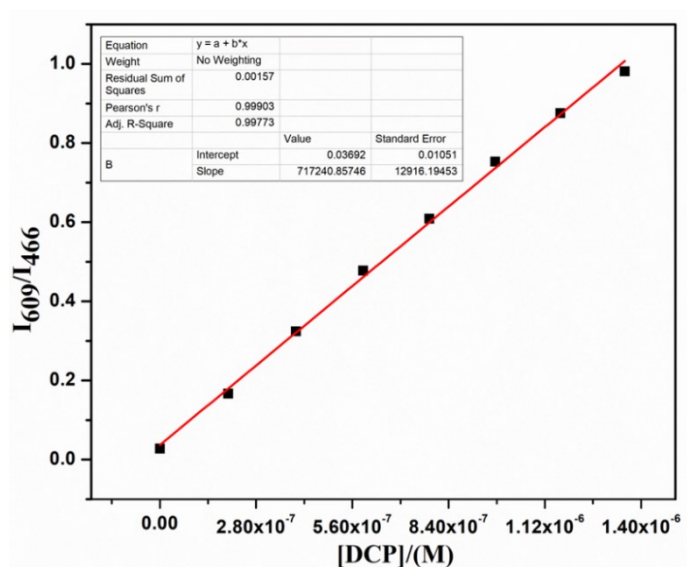


Figure S8: From the graph we get slope (S) = 7.17×10^5 , thus using the formula we obtained the detection limit 1.4×10^{-9} M.

6. pH study:

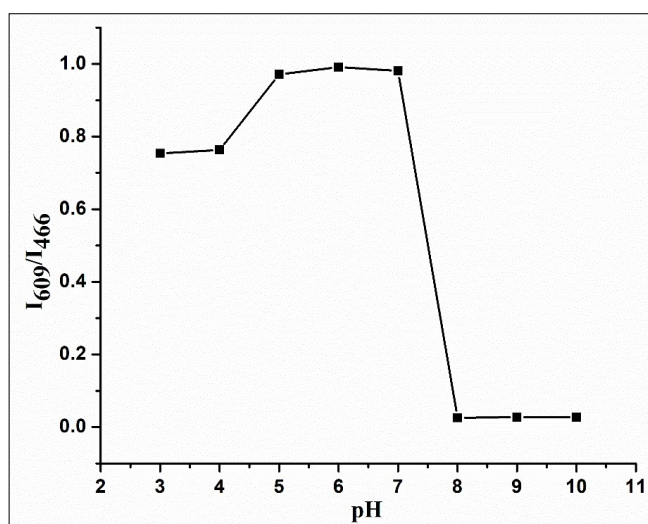


Figure S9: Fluorescence response of PPID at the intensity ratio (I_{609}/I_{466}) as a function of pH in DMSO/H₂O (2/3, v/v) solution. $\lambda_{ex} = 413$ nm

7. Response time:

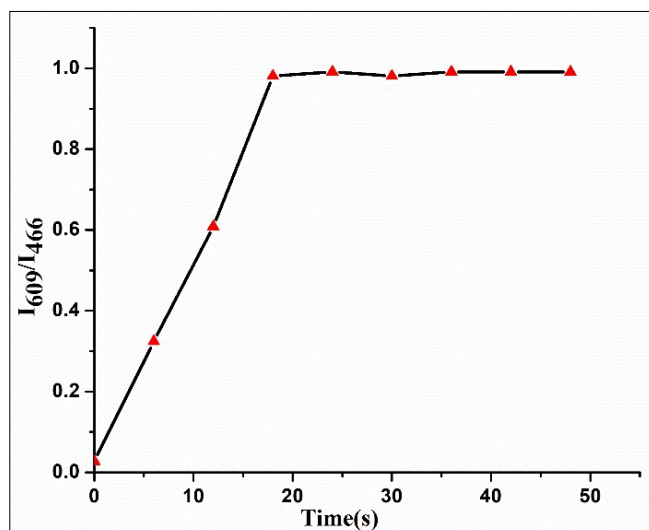


Figure S10: Time-dependent Fluorescence response of the probe in the presence of excess (80 μ L) DCP.

8. Spectral study of CC1:

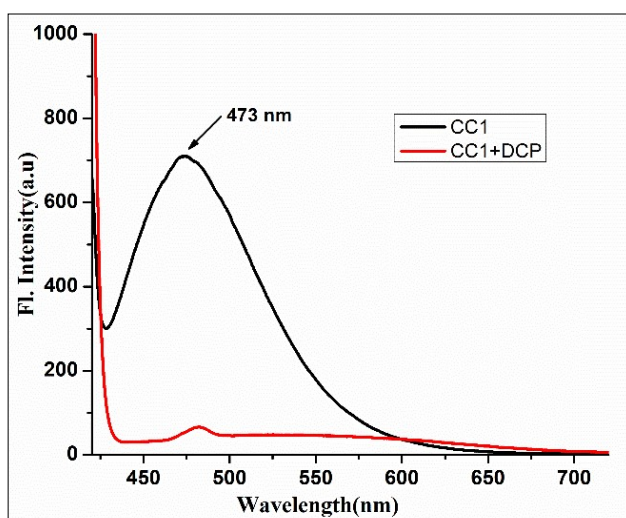


Figure S11: Change in the emission of the compound CC1 in the presence of DCP in the solvent mixture (DMSO/H₂O, 2:3). λ_{ex} = 413 nm

9. HRMS spectra of adduct and controlled compound and 1H NMR of controlled compound:

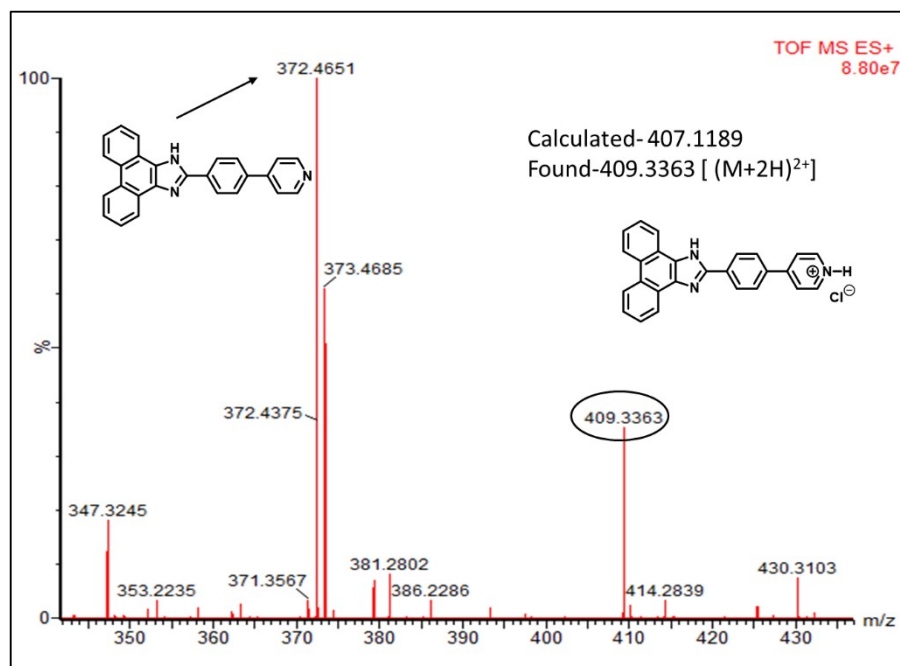


Figure S12: HRMS of adduct PPIDH

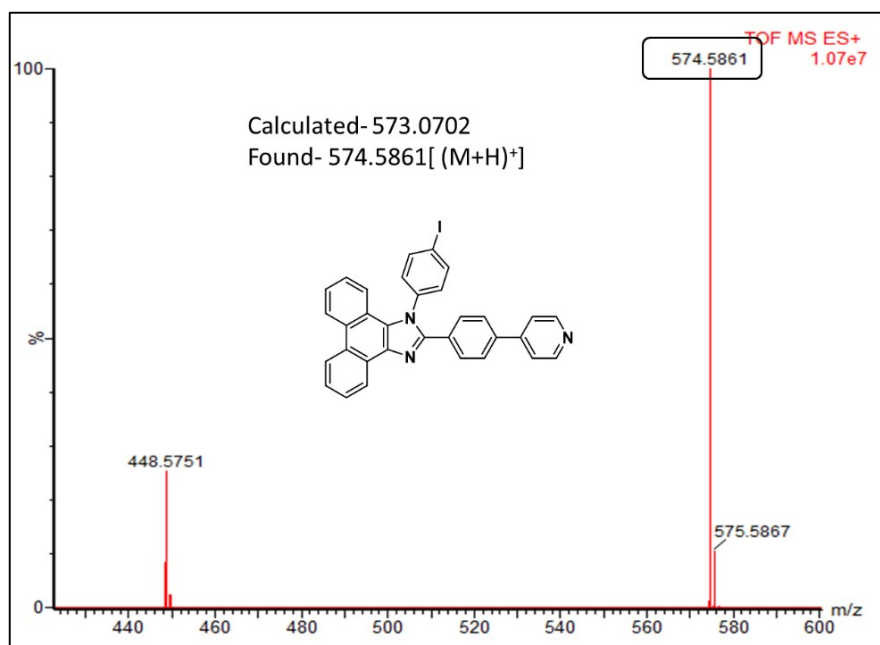


Figure S13: HRMS of the controlled compound CC1

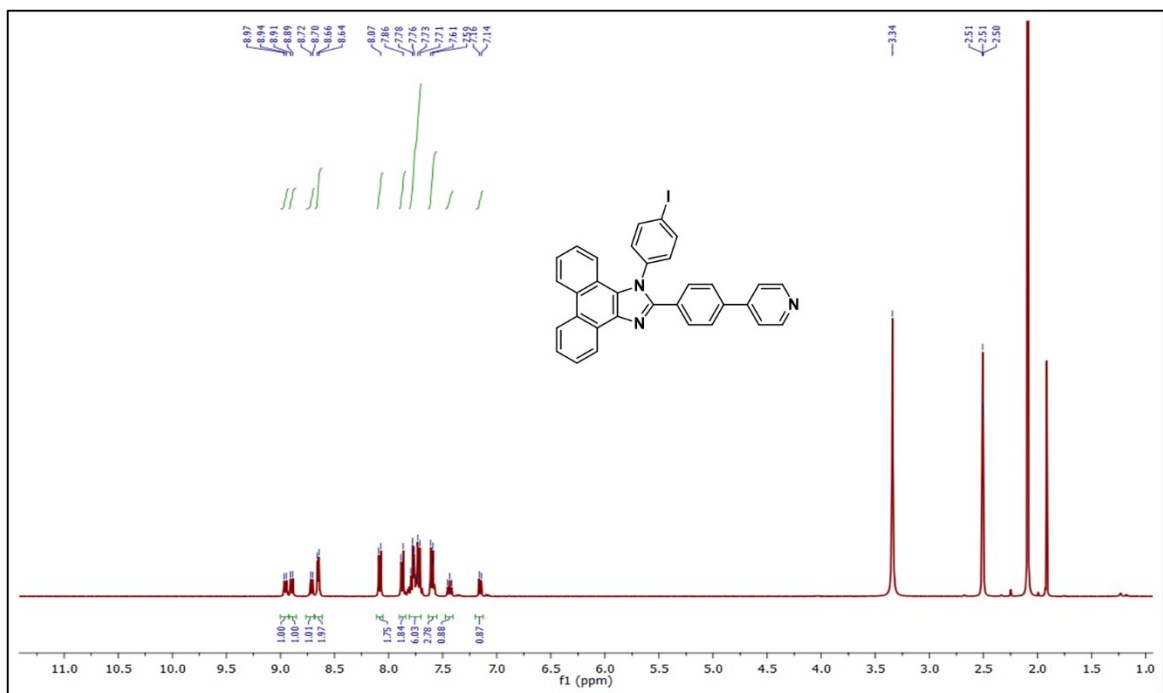


Figure S14: ¹H NMR of the controlled compound CC1

10. Table S4: Crystal Data and Structure Refinement Parameters

Empirical formula	C ₅₂ H ₄₀ N ₆ O ₃
Formula Weight	796.90
Temperature (K)	250
Wavelength (Å)	0.71073
Crystal system	Triclinic
space group	P $\bar{1}$
a, b, c (Å)	11.8392(16), 12.4584(19), 16.460(2)
α , β , γ (°)	104.498(4), 96.983(5), 115.518(4)
Volume (Å ³)	2046.8(5)
Z / Density (calc.) (Mg/m ³)	2/ 1.293
Absorption coefficient (mm ⁻¹)	0.082
F(000)	836.0
Crystal size (mm ³)	0.19 x 0.16 x 0.09

θ range for data collection	2.316 to 27.141
Completeness to θ (%)	100%
Absorption correction	Multi-scan
Max. and min. transmission	0.993 and 0.985
Refinement method	Full-matrix least-squares on F^2
Data/parameters	9062/ 533
Goodness-of-fit on F^2	1.052
Final R indices [$I > 2\sigma(I)$]	$R_1 = 0.0688$, $wR_2 = 0.1856$
R indices (all data)	$R_1 = 0.0992$, $wR_2 = 0.2156$
Largest diff. peak and hole ($e.\text{\AA}^{-3}$)	0.247 and -0.225

$$R_1 = \frac{\sum ||F_o| - |F_c||}{\sum |F_o|}, wR_2 = \left[\frac{\sum \{(F_o^2 - F_c^2)^2\}}{\sum \{w(F_o^2)^2\}} \right]^{1/2} w = 1 / \{ \sigma^2(F_o^2) + (aP)^2 + bP \}, P = (F_o^2 + 2F_c^2) / 3, \text{ where, } a = 0.1183 \text{ and } b = 0$$

11. Cell line study:

Cytotoxicity assay:

In the present study Human breast cancer cell line MDA-MB 231 and human normal kidney epithelial cell line NKE have been used and to assess the cytotoxic effect of the ligand PPID MTT cell proliferation assay¹⁰ was performed. In brief, cells growing in a log phase were first seeded in 96-well plates and were incubated overnight at 37 °C under 5% CO₂. Different working concentration of ligand PPID was prepared using solvent DMSO and H₂O at a ratio of 2:3 and the cells were then exposed to the ligand PPID (0 μ M, 10 μ M, 20 μ M, 40 μ M, 80 μ M, 100 Mm) for 24 hrs. Following incubation, 0.5 mg/ml of MTT solution was added to each well and incubated for 4h, and the cells were then rinsed with 1X PBS. The formazan crystals that formed were then dissolved in DMSO, and the absorbance was measured at 570 nm using a microplate reader. Cell viability was calculated as a percentage of the experimental design used as the control.

Cellular imaging

Fluorescence imaging was carried out in MDA-MB 231 cell line to visualise the ligand **PPID** fluorescence properties when DCP was present. Briefly, cells were cultured on coverslips for 24 hours in a humidified incubator at 37°C with 5% CO₂ before being mock-treated or treated with 10 μ M of the ligand PPID in the presence or absence of 10 μ M DCP individually, and incubated for 15 min and 30 min at 37°C. The cells were first washed with 1 PBS, placed on a glass slide, and then seen using a DAPI filter under an Olympus fluorescence microscope¹¹.

MDA-MB 231 and NKE cell lines were used to test the in-vivo cell Cytotoxicity assay of the ligand PPID. Data from the MTT experiment showed no detectable toxicities even at a concentration of 100 μM of the ligand PPID (Fig-S15B). Hence ligand PPID was chosen to conduct further research at a working concentration of 10 μM .

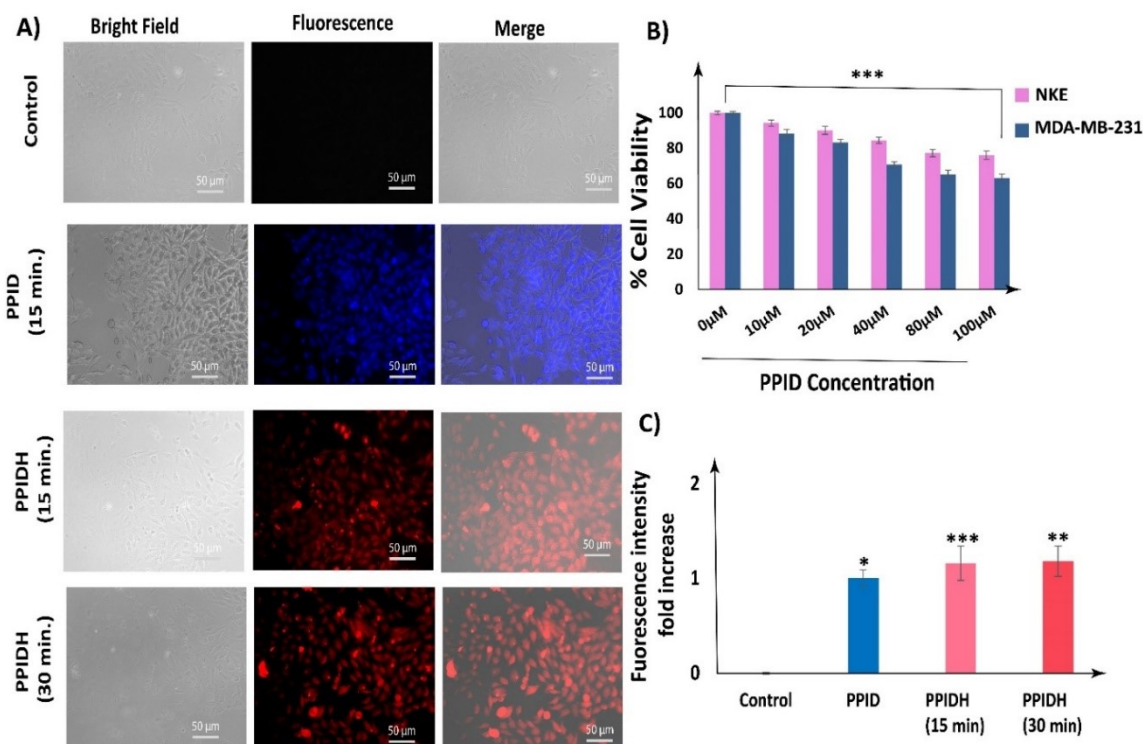


Figure S15: (A) Microscopic images and (C) fold increase in fluorescence intensity of untreated MDA-MB 231 cells (Control), cells treated with ligand PPID (10 μM), [ligand PPID (10 μM) + DCP (10 μM)] PPIDH after the 15 min and after the 30 min, incubation period under bright, fluorescence and merged field. (B) Cell survivability of MDA-MB 231 and NKE cells exposed to different ligand PPID concentration. Data are representative of at least three independent experiments and bar graph shows mean \pm SEM, * $p < 0.0001$, ** $p < 0.001$, *** $p < 0.01$ were interpreted as statistically significant, as compared with the control.

When MDA-MB 231 cells were exposed to the ligand **PPID** (10 μM) alone, an increased level of fluorescence intensity at an emission level of 466 nm have been observed as compared to untreated cells. But, when MDA-MB 231 cells were exposed to the ligand **PPID** (10 μM) in combination with DCP (10 μM) at an incubation time frame of 15 min and 30 min, results from

fluorescence microscopy imaging demonstrated a change in the level of fluorescence intensity at an emission level of 609 nm as compared to the cell exposed to the ligand **PPID** alone (Fig-S15A & C). Consequently, we might draw the conclusion that the cells consume the ligand **PPID** in the presence of DCP and also justified that in the presence of DCP, ligand **PPID** results in shift in the level of fluorescence intensity from blue fluorescent luminescence to red fluorescent luminescence is not an artifact of one of either added compounds. Therefore, as designed our probe **PPID** is biocompatible and conducive to biological application.

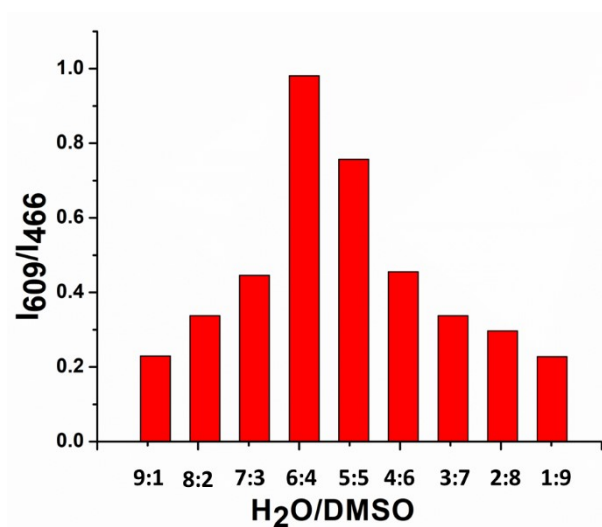


Figure S16: Fluorescence intensity ratio (I_{609}/I_{466}) of PPID (10 μ M) with addition of excess DCP in different ratio of H₂O/DMSO (form 9:1 to 1:9, v/v) and the excitation wavelength was 413 nm.

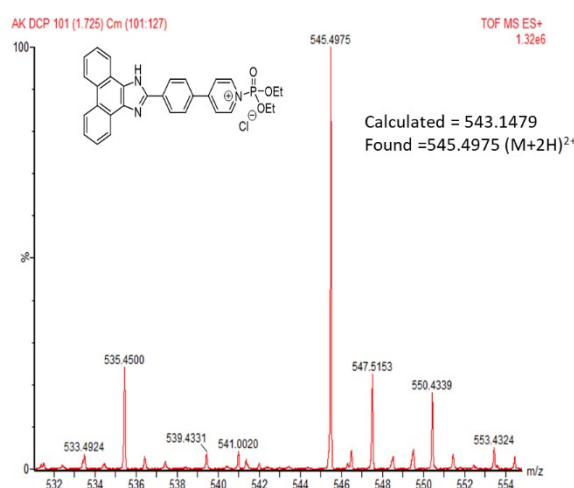


Figure S17: HRMS of the intermediate compound.

References

1. Z. Lu, W. Fan, X. Shi, C. A. Black, C. Fan, and F. Wang, *Sens. Actuators B Chem.*, 2018, **255**, 176-182.
2. S. S. Ali, A. Gangopadhyay, A. K. Pramanik, U. N. Guria, S. K. Samanta, and A. K. Mahapatra, *Dyes Pigm.*, 2019, **170**, 107585.
3. T. I. Kim, S. B. Maity, J. Bouffard, and Y. Kim, *Anal. Chem.*, 2016, **88**, 9259-9263.
4. S. Goswami, A. Manna and S. Paul, *RSC Adv.*, 2014, **4**, 21984-21988.
5. H. Xu, H. Zhang, L. Zhao, C. Peng, G. Liu and T. Cheng, *New New J. Chem.*, 2020, **44**, 10713-10718.
6. U. N. Guria, K. Maiti, S. S. Ali, A. Gangopadhyay, S. K. Samanta, K. Roy and A. K. Mahapatra, *ChemistrySelect*, 2020, **5**, 3770-3777.
7. T. Qin, Y. Huang, K. Zhu, J. Wang, C. Pan, B. Liu and L. Wang, *Anal. Chim. Acta*, 2019, **1076**, 125-130.
8. K. Aich, S. Das, S. Gharami, L. Patra and T. K. Mondal, *New New J. Chem.*, 2017, **41**, 12562-12568.
9. J. Yao, Y. Fu, W. Xu, T. Fan, Y. Gao, Q. He and J. Cheng, *Anal. Chem.*, 2016, **88**, 2497-2501.
10. P.R. Twentyman and M. Luscombe, *Br. J. Cancer*, 1987, **56**, 279-285.
11. M. Mandal, D. Sain, M.M. Islam, D. Banik, M. Periyasamy, S. Mandal, A.K. Mahapatra, and A. Kar, *Anal. Methods*, 2021. **13**, 3922-3929.